

# Frequency Response Analysis of Active Disturbance Rejection Based Control System

Gang Tian<sup>1</sup> and Zhiqiang Gao<sup>1,2</sup>

**Abstract**—Active Disturbance Rejection is a relatively new, and quite different, design concept that shows much promise in obtaining consistent response in an industrial control system full of uncertainties. But most of the development and analysis has previously been shown in the time-domain. In this paper, frequency-domain analysis of such a control system is performed to quantify its performance and stability characteristics. The transfer function description of the controller is derived and, together with a highly uncertain linear time-invariant plant, the loop gain frequency response is analyzed. The result shows that the active disturbance rejection based control system possesses a high level of robustness. The bandwidth and stability margins, in particular, are nearly unchanged as the plant parameters vary significantly; so is the sensitivity to input disturbance. Such characteristics makes this control system an appealing solution in dealing with real world control problems where uncertainties abound.

**Index Terms**—Active Disturbance Rejection, Stability Margins, Robustness.

## I. INTRODUCTION

Simple and effective, the Proportional-Integral-Derivative (PID) controller has flourished in industry [1]. But the ever increasing demands on accuracy, robustness, and efficiency, coupled with the inherent limitations of PID, have driven engineers to seek better control mechanisms elsewhere. In recent years, a promising new control design framework, the Active Disturbance Rejection Control (ADRC), has emerged as a viable alternative. It offers a timely, if not conventional, solution to practical problems.

The ADRC as a design method was first proposed by J. Han in 1990s [2]- [5]. The active disturbance rejection concept was first introduced in the English literature in [6] and further simplified and explicated in [7] and [8], respectively. The central idea is that both the internal dynamics and the external disturbances can be estimated and compensated for in real time. This is a drastic departure from the existing model-based design paradigm since the information of the physical process needed by the controller is obtained from the plant input-output data in real time, not from an *a priori* mathematical model. This new design framework applies generally to nonlinear and time varying systems with single-input and single-output (SISO) or multiple-input and multiple-output (MIMO).

The active disturbance rejection concept is deceptively simple, as will be shown in the next section. Its remarkable

robustness against dynamic variations and external disturbances, inherent due to the fact that this controller is not dependent upon an accurate mathematical model of the plant, is demonstrated in practical applications time and again [11], [12]- [14]. But as ADRC becomes more widely used, it is of significant importance that the new framework is understood using the almost universal frequency response language shared by practicing control engineers: bandwidth, and stability margins, etc. Such language is taught in every basic control course. See, for example, the textbook [9].

ADRC was originally formulated using nonlinear gains, which makes the frequency response analysis difficult. To evaluate the disturbance rejection property, a sinusoidal sweep was used in [10] to obtain the approximate frequency response, a quite cumbersome task. The simplification of ADRC in [7] using linear and parameterized gains provides a much needed, easy to implement, formulation. More importantly, it enables a thorough evaluation of ADRC in the frequency domain. In particular, the work in [7] allows ADRC to be represented in transfer function form. Together with a linear plant with uncertain parameters, the loop gain frequency response will be able to show the robustness of the control system.

The paper is organized as follows. In Section II, the concept of the Active Disturbance Rejection is briefly introduced, followed by the derivation of its transfer function description. Section III begins with the stability investigation of ADRC, followed by the robustness analysis of ADRC. Concluding remarks are given in section IV.

## II. TRANSFER FUNCTION REPRESENTATION OF ADRC

### A. The Idea of Active Disturbance Rejection

Consider a general second-order plant:

$$\ddot{y} = f(y, \dot{y}, w, t) + bu \quad (1)$$

where  $y$  is the system output,  $u$  is the control signal,  $b$  is a constant, and  $w$  represents external disturbances. In the ADRC framework, the entire  $f(y, \dot{y}, w, t)$  is assumed unknown and denoted as the *generalized disturbance*. It is the combination of the internal dynamics of the system and external disturbances. If the *generalized disturbance* can be estimated and cancelled, the system is then reduced to a simple double-integral plant with a scaling factor  $b$ , simplifying the control problem. The estimation problem of  $f(y, \dot{y}, w, t)$  leads us to a unique state observer known as the Extended State Observer (ESO).

The state space model of (1) is augmented to include an additional state  $f(y, \dot{y}, w, t)$ , or simply  $f$ . Let  $x_1 = y$ ,  $x_2 =$

<sup>1</sup>Center for Advanced Control Technologies, Department of Electrical and Computer Engineering, Cleveland State University, Cleveland, OH 44115, USA

<sup>2</sup>The Corresponding author. E-mail: z.gao@ieee.org. Tel:1-216-687-3528, Fax:1-216-687-5405

$\dot{y}$ ,  $x_3 = f$ . Assuming  $f$  is differentiable, and let  $h = \dot{f}$ . The augmented model of (1) is

$$\begin{cases} \dot{x} = Ax + Bu + Eh \\ y = Cx \end{cases} \quad (2)$$

where:

$$A = \begin{bmatrix} 0 & 1 & 0 \\ 0 & 0 & 1 \\ 0 & 0 & 0 \end{bmatrix}, B = \begin{bmatrix} 0 \\ b \\ 0 \end{bmatrix}, E = \begin{bmatrix} 0 \\ 0 \\ 1 \end{bmatrix},$$

and  $C = [1 \ 0 \ 0]$ . The ESO is a state observer of the augmented plant:

$$\begin{cases} \dot{z} = Az + Bu + L(x_1 - z_1) \\ \hat{y} = Cz \end{cases} \quad (3)$$

where the observer gain vector  $L$  is chosen such that all the observer eigenvalues are located at  $-w_o$ . That is

$$L = [3\omega_o \ 3\omega_o^2 \ \omega_o^3]^T$$

This makes  $w_o$  the only tuning parameter for the ESO [7].

With a well-tuned observer,  $z_1$ ,  $z_2$  and  $z_3$  closely track  $y$ ,  $\dot{y}$ , and  $f$  respectively. The control law

$$u = (u_0 - z_3) / b \quad (4)$$

reduces the original plant roughly to a double-integral plant

$$\ddot{y} = u_0 \quad (5)$$

which can be easily controlled by a Proportional-Derivative (PD) controller

$$u_0 = k_p(r - z_1) - k_d z_2 \quad (6)$$

The controller gains  $k_p$  and  $k_d$  are chosen as  $\omega_c^2$  and  $2\omega_c$ , respectively, placing all the closed-loop poles at  $-\omega_c$ . Thus the number of the tuning parameters in the controller is reduced to one [7].

### B. Transfer Function Derivation

Consider a linear time-invariant second-order plant:

$$\ddot{y} = -a_1 \dot{y} - a_0 y + bu \quad (7)$$

with  $a_0$  and  $a_1$  unknown, and  $f = -a_1 \dot{y} - a_0 y$  in this particular case. Since both the plant and the controller are linear, the robustness of the control system can be evaluated using frequency response. If ADRC indeed estimates  $f$  and cancels it out, then we should see very little changes in bandwidth and stability margins when  $a_0$  and  $a_1$  vary. To verify this prediction using the frequency response, we need the loop gain transfer function.

The transfer function of (7) is:

$$G_p(s) = \frac{b}{s^2 + a_1 s + a_0} \quad (8)$$

The transfer functions of the ADRC can be derived in the form of a two-degree-of-freedom (2dof) closed-loop system, as shown in Fig.1, where  $G_p(s)$  represents the transfer function of the plant,  $R(s)$ ,  $U(s)$ , and  $Y(s)$  are the reference

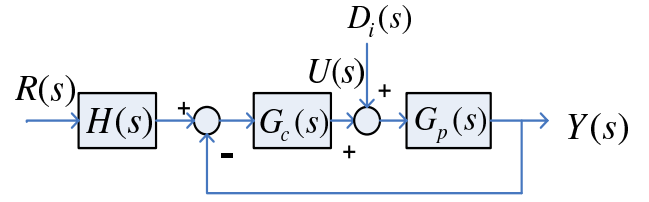


Fig. 1. Block Diagram of the system in Transfer Function Form of ADRC

signal, control signal, and output respectively;  $D_i(s)$  is the input disturbance.

Converting the ADRC equations to the frequency domain using the Laplace transform, the 2dof transfer functions are

$$G_c(s) = \frac{1}{b_0 s} \frac{C_{n2}s^2 + C_{n1}s + C_{n0}}{C_{d2}s^2 + C_{d1}s + C_{d0}} \quad (9)$$

$$H(s) = \omega_c^2 \frac{H_{n3}s^3 + H_{n2}s^2 + H_{n1}s + H_{n0}}{H_{d2}s^2 + H_{d1}s + H_{d0}} \quad (10)$$

where the coefficients in (9) and (10) are listed in the appendix. From these transfer functions, the loop gain transfer function  $G_{lg}(s)$  and the closed-loop system transfer function  $G_{YR}(s)$  are readily available:

$$G_{lg}(s) = G_p(s)G_c(s) \quad (11)$$

$$G_{YR}(s) = \frac{Y(s)}{R(s)} = \frac{H(s)G_c(s)G_p(s)}{1 + G_c(s)G_p(s)} \quad (12)$$

Furthermore, the transfer function from the input disturbance to the output is

$$G_{YD_i}(s) = \frac{G_p(s)}{1 + G_c(s)G_p(s)} \quad (13)$$

From these transfer functions, the frequency analysis will proceed.

### III. FREQUENCY RESPONSE

Consider a particular motion control example, where the plant in (7) comes with the parameters of  $a_0 = 0$ ,  $a_1 = 3.085$ , and  $b = 206.25$ , and a particular ADRC designed with  $\omega_o = \omega_c = 100$  rad/sec.

#### 1) Bandwidth and Stability:

The stability of a closed-loop transfer function is determined by the pole locations of (12). Since  $H(s)$  is guaranteed stable, because all three coefficients in its denominator are positive, the closed-loop stability can be determined from the poles of  $\frac{G_c(s)G_p(s)}{1 + G_c(s)G_p(s)}$ , whose characteristic polynomial is

$$A_{cl}(s) = s^5 + A_4 s^4 + A_3 s^3 + A_2 s^2 + A_1 s + A_0 \quad (14)$$

(The coefficients in (14) are also listed in the appendix.) The question is, given an ADRC controller, for what range of  $a_0$  and  $a_1$  the closed-loop system is stable?

For simplicity, the bandwidths of the controller and the observer in ADRC are chosen as the same:  $\omega_c = \omega_o$ . Finding the analytical solution using Routh-Hurwitz criterion is

complex for this problem. Instead, a search program is used to determine the region in  $a_0$ - $a_1$  plane where the closed-loop system is stable. And this is repeated for different  $\omega_o = \omega_c$ . The results are shown in Fig.2, where the area to the upper-right side of the curve is the stable region.

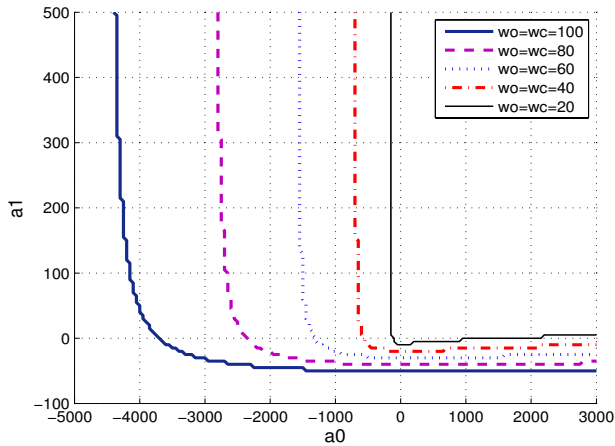


Fig. 2. Stability in  $a_0$ - $a_1$  plane

Fig.2 shows that as the bandwidth,  $\omega_o = \omega_c$ , increases, the stable area in  $a_0$ - $a_1$  plane is expanded, particularly to the left on the  $a_0$  axis. It also shows that even if the plant is unstable (either  $a_0$  or  $a_1$  is negative), the closed-loop system can still be made stable, given enough controller and observer bandwidth. In other words, the higher the bandwidth, the more parametric uncertainties the system can tolerate.

## 2) Loop Gain Frequency Response:

The Bode plots of the loop gain transfer function are shown in Fig.3, with  $\omega_c = \omega_o = 100$  rad/sec,  $b = 206.25$ ,  $a_1 = 3.085$ , and  $a_0 = [0, 0.1, 1, 10, 100]$ . The stability margins for each curve in Fig.3 are shown in TABLE I. Fig.3 and TABLE I show that, remarkably, gain margin, phase margin and cross-over frequency are almost immune to changes in  $a_0$ .

TABLE I  
GAIN MARGIN AND PHASE MARGIN UNDER DIFFERENT  $a_0$

	neg GM dB (rad/sec)	pos GM	PM deg(rad/sec)
$a_0=0$	-13.0 (34)	11.7 (276)	33.7 (100)
$a_0=0.1$	-13.0 (34)	11.7 (276)	33.7 (100)
$a_0=1$	-12.9 (34)	11.7 (276)	33.7 (100)
$a_0=10$	-13.1 (34)	11.7 (276)	33.7 (100)
$a_0=100$	-13.9 (33)	11.7 (276)	33.7 (101)

Similarly, the Bode plots of the loop gain transfer function are shown in Fig.4, with  $\omega_c = \omega_o = 100$  rad/sec,  $b = 206.25$ ,  $a_0 = 0$ , and  $a_1 = [0.1, 1, 3.085, 10, 100]$ . The stability margins for each curve in Fig.4 are shown in TABLE II. Fig.4 and TABLE II show that the gain margin, phase margin, and

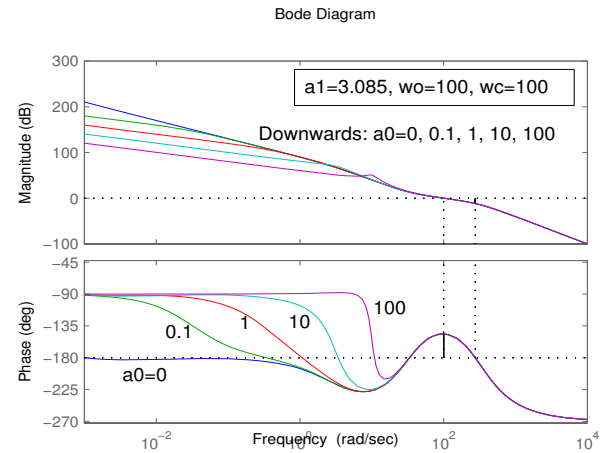


Fig. 3. Loop Gain Bode Plots for  $a_0 = [0, 0.1, 1, 10, 100]$

cross-over frequency are just as insensitive to changes in  $a_1$  as to those in  $a_0$ .

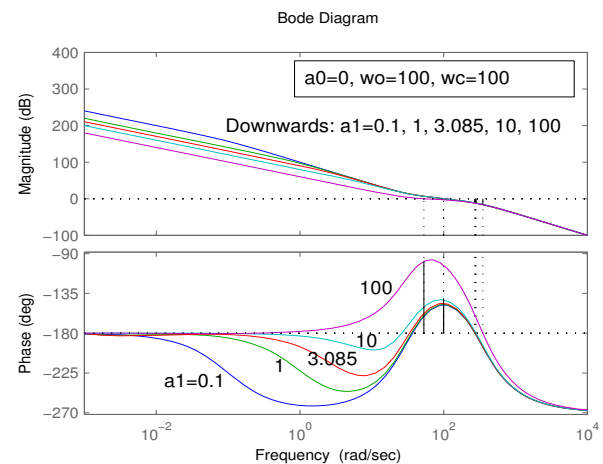


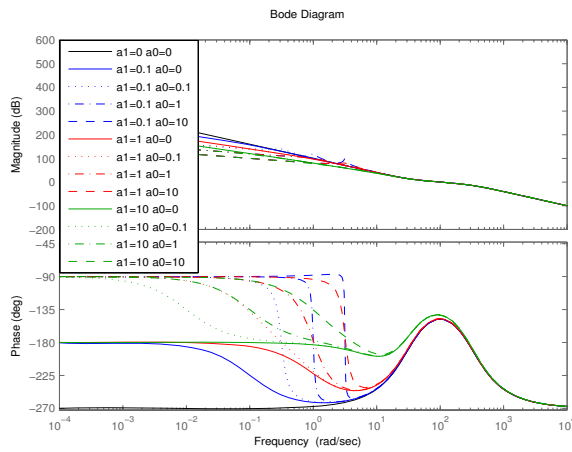
Fig. 4. Loop Gain Bode Plots for  $a_1 = [0.1, 1, 3.085, 10, 100]$

TABLE II  
GAIN MARGIN AND PHASE MARGIN UNDER DIFFERENT  $a_1$

	neg GM dB (rad/sec)	pos GM	PM deg(rad/sec)
$a_1=0.1$	-11.6 (36.5)	11.6 (273)	31.9 (100)
$a_1=1$	-12.0 (35.7)	11.6 (274)	32.5 (100)
$a_1=3.085$	-13.0 (33.6)	11.7 (276)	33.7 (100)
$a_1=10$	-16.9 (26.2)	12.1 (282)	37.6 (99.6)
$a_1=100$	N/A	16.2 (352)	81.2 (53.2)

As for uncertainties in the plant parameter  $b$ , the gain margins indicate that the upper and lower limits for the acceptable variations.

Finally,  $a_0$  and  $a_1$  are changed simultaneously, as shown in Fig.5. Again, similar to Fig.3 and Fig.4, the gain margin, phase margin, and cross-over frequency change very little for different combinations of  $a_0$  and  $a_1$ .

Fig. 5. Loop Gain Bode plots for different  $a_1$  and  $a_0$ 

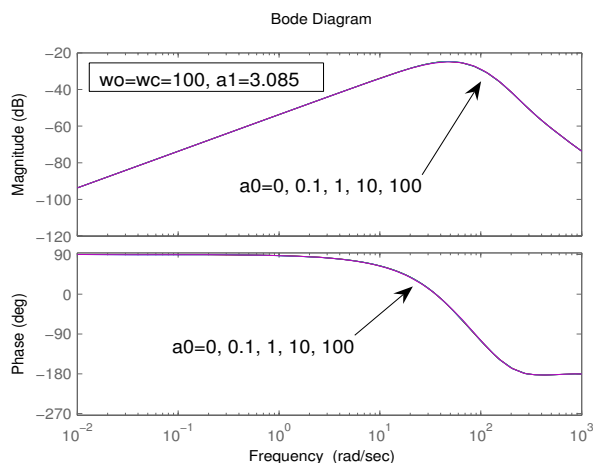
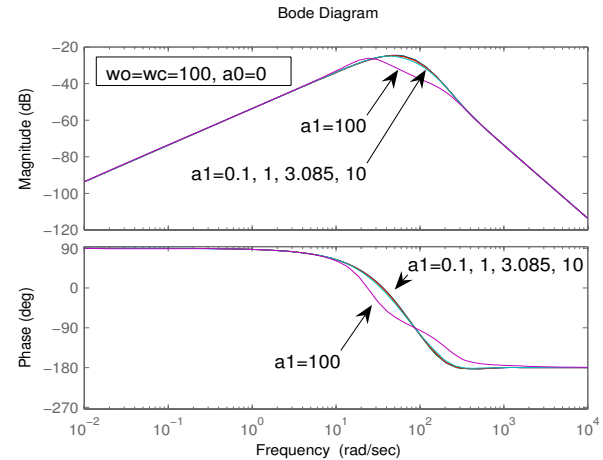
### 3) External Disturbance Rejection:

In this section it will be shown that consistent input disturbance rejection is achieved even in the presence of significant uncertainties of  $a_0$  and  $a_1$ . First, the transfer function between the input disturbance and the output is obtained by substituting (8) and (10) into (13):

$$G_{YD_i}(s) = \frac{bs(C_{d2}s^2 + C_{d1}s + C_{d0})}{A_{cl}(s)} \quad (15)$$

where  $A_{cl}(s)$  is a fifth-order polynomial with non-zero coefficient of  $s^0$ , as shown in (14). Equation (15) shows that  $G_{YD_i}(s)$  tends to 0 when  $s$  approaches zero and when  $s$  approaches  $\infty$ . What is interesting to find out is how it behaves in the mid range of frequencies and how it is affected by parametric uncertainties in  $a_0$  and  $a_1$ .

The Bode plots of (15) are shown in Fig.6 and Fig.7, respectively, demonstrating excellent disturbance rejection properties that are unaffected by the plant parametric uncertainties.

Fig. 6. Bode plots of  $G_{YD_i}(s)$  for  $a_0 = [0, 0.1, 1, 10, 100]$ Fig. 7. Bode plots of  $G_{YD_i}(s)$  for  $a_1 = [0.1, 1, 3.085, 10, 100]$ 

## IV. CONCLUDING REMARKS

In this paper, the transfer function description is obtained for the ADRC-based control system that, until now, has mainly been developed and analyzed in the time-domain. This description allows the ADRC to be evaluated, against a 2<sup>nd</sup>-order SISO linear time invariant (LTI) plant with parametric uncertainties, using the classical transfer function and frequency response techniques. Explaining and examining a new control concept in a language practicing engineers are familiar with proves to be effective. It is shown that stability robustness in the presence of parametric uncertainties clearly improves as the controller and observer bandwidth increases. More importantly, the loop gain frequency response shows a remarkable level of consistency in bandwidth and stability margins against significant parameter variations in the plant. Similar consistency is also found in the disturbance rejection performance.

Although ADRC is generally applicable to nonlinear, time-varying,  $n^{\text{th}}$ -order systems with multiple-input and multiple-output, applying it to a SISO LTI plant demonstrates how powerful the new idea is. Many modern control techniques reduce to an equivalent classical loop-shaping design with no improvement, when they are applied to a SISO LTI plant. ADRC proves otherwise. It even produces a much better solution for SISO design. The promise of estimating and canceling the *generalized disturbance* in the time-domain formulation of ADRC is convincingly confirmed in this frequency response analysis.

Future research can be extended from this work. First, with the derived 2dof transfer functions, robustness analysis of ADRC can be performed by applying small gain theorem, in which ADRC can be interpreted in the modern robust control. Second, frequency response analysis of ADRC can be carried out for systems more complex than the second-order system investigated in this analysis, even MIMO systems.

## APPENDIX

TABLE III  
COEFFICIENTS IN  $C(s)$ ,  $H(s)$  AND  $A_{cl}(s)$

$C_{n2} = 3\omega_c^2\omega_o + 6\omega_c\omega_o^2 + \omega_o^3$	$C_{d2} = 1$
$C_{n1} = 3\omega_c^2\omega_o^2 + 2\omega_c\omega_o^3$	$C_{d1} = 2\omega_c + 3\omega_o$
$C_{n0} = \omega_c^2\omega_o^3$	$C_{d0} = \omega_c^2 + 3\omega_o^2 + 6\omega_c\omega_o$
$H_{n3} = 1$	
$H_{n2} = 3\omega_o$	$H_{d2} = C_{n2}$
$H_{n1} = 3\omega_o^2$	$H_{d1} = C_{n1}$
$H_{n0} = \omega_o^3$	$H_{d0} = C_{n0}$
$A_4 = a_1 + C_{d1}$	$A_3 = a_0 + a_1C_{d1} + C_{d0}$
$A_2 = a_0C_{d1} + a_1C_{d0} + b/b_0C_{n2}$	$A_1 = a_0C_{n2} + b/b_0C_{n1}$
$A_0 = b/b_0C_{n0}$	

## REFERENCES

- [1] K. J. Astrom, T. Hagglund, *PID Controllers: Theory, Design, and Tuning*, International Society for Measurement and Con, 1995.
- [2] J. Han, "A class of extended state observers for uncertain systems," *Control and Decision*, vol. 10, no. 1, pp. 85-88, 1995. (In Chinese)
- [3] J. Han, "Nonlinear state error feedback control," *Control and Decision*, vol. 10, no. 3, pp. 221-225, 1995. (In Chinese)
- [4] J. Han, "Auto-disturbance rejection control and its applications," *Control and Decision*, vol. 13, no. 1, pp. 19-23, 1998. (In Chinese)
- [5] J. Han, "Nonlinear design methods for control systems," *Proc. of the 14th IFAC World Congress*, 1999.
- [6] Z. Gao, Y. Huang, and J. Han, "An alternative paradigm for control system design," *Proc. of IEEE conference on Decision and Control*, Volume 5, 4-7 Dec. 2001 Page(s):4578 - 4585
- [7] Z. Gao "Scaling and Parameterization Based Controller Tuning," *Proc. of the 2003 American Control Conference*, Volume 6, 4-6 June 2003 Page(s):4989 - 4996
- [8] Z. Gao, "Active disturbance rejection control: a paradigm shift in feedback control system design," *Proc. of the 2006 American Control Conference*, pp. 2399-2405, 2006.
- [9] BC Kuo, *Automatic Control Systems*, Prentice Hall, 7th ed. 1995
- [10] Z. Gao, S. H., F. Jiang "A Novel Motion Control Design Approach Based on Active Disturbance Rejection." *IEEE Conference on Decision and Control*. Volume 5, 4-7 Dec. 2001 Page(s):4877 - 4882
- [11] Z. Gao, S. Hu, and F. Jiang, "A novel motion control design approach based on active disturbance rejection," *Proceedings of IEEE Conference on Decision and Control*, Volume 5, 4-7 Dec. 2001 Page(s):4877 - 4882
- [12] Y. Hou, Z. Gao, F. Jiang, and B. Boulter, "Active Disturbance Rejection Control for Web Tension Regulation", *IEEE CDC conference*, Volume 5, 4-7 Dec. 2001 Page(s):4974 - 4979
- [13] F. Goforth, "On Motion Control Design and Tuning Techniques," *Proc. of the 2004 American Control Conference*, Boston, Volume 1, 30 June-2 July 2004 Page(s):716 - 721
- [14] Y. X. Su, B. Y. Duan, C.H. Zheng, Y. F. Zhang, G. D. Chen, and J. W. Mi, "Disturbance-Rejection High-Precision Motion Control of a Stewart Platform", *IEEE Transactions on Control System Technology*, Vol. 12, Issue 3, May 2004 Page(s):364 - 374